Received: 6 December 2021 | Revised: 14 May 2022 | Accepted: 25 May 2022

DOI: 10.1111/cas.15444

ORIGINAL ARTICLE

Cancer Science WILEY

Prosaposin, tumor-secreted protein, promotes pancreatic cancer progression by decreasing tumor-infiltrating lymphocytes

Yoji Miyahara[1] | Shigetsugu Takano[1] | Kazuyuki Sogawa[2] | Satoshi Tomizawa[1] | Katsunori Furukawa[1] | Tsukasa Takayashiki[1] | Satoshi Kuboki[1] | Masayuki Ohtsuka[1]

[1]Department of General Surgery, Graduate School of Medicine, Chiba University, Chiba, Japan

[2]Department of Biochemistry, School of Life and Environmental Science, Azabu University, Kanagawa, Japan

Correspondence
Shigetsugu Takano Department of General Surgery, Graduate School of Medicine, Chiba University, 1-8-1, Inohana, Chuo-ku, Chiba 260-8677, Japan.
Email: stakano@faculty.chiba-u.jp

Funding information
Grant-in-Aid for Scientific Research (KAKENHI), Grant/Award Number: 19H03725 and 19K09113

Abstract

Glycoproteins produced by tumor cells are involved in cancer progression, metastasis, and the immune response, and serve as possible therapeutic targets. Considering the dismal outcomes of pancreatic ductal adenocarcinoma (PDAC) due to its unique tumor microenvironment, which is characterized by low antitumor T-cell infiltration, we hypothesized that tumor-derived glycoproteins may serve as regulating the tumor microenvironment. We used glycoproteomics with tandem mass tag labeling to investigate the culture media of three human PDAC cell lines, and attempted to identify the key secreted proteins from PDAC cells. Among the identified glycoproteins, prosaposin (PSAP) was investigated for its functional contribution to PDAC progression. PSAP is highly expressed in various PDAC cell lines; however, knockdown of intrinsic PSAP expression did not affect the proliferation and migration capacities. Based on the immunohistochemistry of resected human PDAC tissues, high PSAP expression was associated with poor prognosis in patients with PDAC. Notably, tumors with high PSAP expression showed significantly lower $CD8^+$ T-cell infiltration than those with low PSAP expression. Furthermore, PSAP stimulation decreased the proportion of $CD8^+$ T cells in peripheral blood monocytes. Finally, in an orthotopic transplantation model, the number of $CD8^+$ T cells in the PSAP shRNA groups was significantly increased, resulting in a decreased tumor volume compared with that in the control shRNA group. PSAP suppresses $CD8^+$ T-cell infiltration, leading to the promotion of PDAC progression. However, further studies are warranted to determine whether this study contributes to the development of a novel immunomodulating therapy for PDAC.

KEYWORDS
antitumor immunity, pancreatic ductal adenocarcinoma, prosaposin, tumor microenvironment, tumor-infiltrating lymphocytes

Abbreviations: Con A, concanavalin A; EMT, epithelial-to-mesenchymal transition; HPFs, high-power fields; IF, immunofluorescence staining; IHC, immunohistochemistry; LRP-1, low-density lipoprotein receptor-related protein-1; PDAC, pancreatic ductal adenocarcinoma; rhPSAP, recombinant human PSAP; TILs, tumor-infiltrating lymphocytes; TLR4, Toll-like receptor 4; TME, tumor microenvironment; TMT, tandem mass tag.

1 | INTRODUCTION

Treatment strategies have been developed for PDAC, however its prognosis is extremely severe, with a 5-year survival rate of ~10% in the USA in 2020.[1] One of the critical reasons for the dismal outcomes in patients with PDAC may lie in the unique TME characterized by dense stroma and low infiltration of antitumor T cells.[2–5] Immunotherapy has been introduced as a novel therapy for malignancies in the last decade and has been attracting wide interest.[6–9] However, its efficacy in PDAC is limited because of the immunosuppressive TME.[10–12]

The TME is mainly composed of cancer cells, stroma, and immune cells. Furthermore, interactions among these components by various molecules are considered to be important in cancer progression. Among these molecules, secreted proteins from cancer cells or fibroblasts play an important role in establishing a cancer-promoting or suppressive environment. Therefore, we hypothesized that the secreted proteins from cancer cells could regulate the TME to improve the antitumor efficacy in PDAC.

Glycoproteins are molecules comprising protein and carbohydrate chains, and are involved in many physiological functions. Glycan modification is a key cellular mechanism considered to be deeply involved in cancer progression including carcinogenesis, metastasis, and the immune response, therefore serving as a possible therapeutic target.[13–16] Tandem mass tag labeling is a comprehensive, quantitative proteomic technique for analyzing secreted proteins.[17] In the present study, we used glycoproteomic techniques with TMT labeling to investigate the supernatant of PDAC cell cultures and identified prosaposin (PSAP) as a PDAC cell-derived secreted protein. PSAP is secreted into the extracellular matrix as a full-length protein with various neurotrophic functions.[18,19] Several studies have reported the function of PSAP in cancer progression,[20–24] however its functional roles in the TME of PDAC remain unclear.

Therefore, we investigated the clinical features and prognostic significance of PSAP in resected PDAC tissues. Furthermore, we examined the functional contributions of PSAP regulation to tumor-infiltrating T cells in the TME of PDAC using in vivo experiments. This study would provide novel insights into the modulation of antitumor immunity by PSAP regulation, indicating its potential for the development of a novel immunotherapy for PDAC.

2 | MATERIALS AND METHODS

2.1 | Human and murine cell lines

Human pancreatic duct epithelial (HPDE) cells and human PDAC cell lines (BxPC-3, PANC-1, MIA PaCa-2, Capan-2, Capan-1, AsPC-1, CFPAC-1, and Hs766T) were purchased from the ATCC. Murine PDAC cell lines (PKCY cells) derived from a genetically engineered PKCY mouse (*Pdx1-cre*; *LSL-Kras*$^{G12D/+}$;*p53*$^{fl/+}$;*R26*^{YFP} mouse) were provided by Dr. Andrew D. Rhim (The University of Texas, MD Anderson Cancer Center).

2.2 | Glycoprotein isolation and TMT labeling

Three human PDAC cell lines (BxPC-3, PANC-1, and MIA PaCa-2) were cultured for 72 h and the culture supernatants were harvested for secretome analysis. To extract glycoproteins, paramagnetic nonporous particles coupled with a *Lens culinaris* lectin ligand (LCA; Bruker Daltonics) were used to process the culture supernatant samples. The binding, washing, and elution procedures were performed according to the manufacturer's instructions.

Reduction, alkylation, and enzymatic in-solution digestion of proteins were performed as previously described.[17] The TMT-sixplex Isobaric Label Reagent Set (90061, Thermo Fisher Scientific) was used for TMT labeling according to the manufacturer's instructions.

2.3 | Liquid chromatography–tandem mass spectrometry (LC–MS/MS) analysis

The peptides were injected into a trap column (C18, 5 μm, 0.3 × 5 mm; DIONEX) and an analytical column (C18, 3 μm, 0.075 × 120 mm; Nikkyo Technos), attached to an Ultimate 3000 system (DIONEX). Purified peptides were introduced into the LTQ-Orbitrap XL (Thermo Scientific), a hybrid ion-trap Fourier transform mass spectrometer, and analyzed using parameters described in a previous study.[25] A database search engine (Proteome Discoverer; Thermo Scientific) was used to identify and quantify proteins from the mass, tandem mass, and reporter ion spectra of the peptides. Peptide mass data were matched by searching the International Protein Index database (IPI).

2.4 | Western blot analysis

Extracted proteins were separated on polyacrylamide gels (DRC) and transferred to PVDF membranes (PerkinElmer). Nonspecific protein blocking was performed using 5% BSA. The membranes were incubated overnight at 4°C with primary antibodies and then incubated with secondary antibodies for 60 min at room temperature. The membranes were subsequently exposed to a chemiluminescent substrate (Nacalai Tesque) and analyzed using a LAS-4000UV image analyzer (Fujifilm).

2.5 | siRNA and shRNA transfection

PSAP-specific siRNAs (J-003694-17-0002, J-003694-18-0002, Dharmacon) and negative control siRNA (Qiagen) were transfected at a concentration of 5 nmol/L using Lipofectamine RNAiMAX Reagent (Invitrogen). Lentiviral transfection of shRNA was conducted (negative control shRNA: SHC016V-1EA, PSAP shRNA-1:

TRCN000105295, and PSAP shRNA-2: TRCN00011792, Merck KGaA).

2.6 | RT-PCR

RNA was extracted from cell lines using the RNeasy Mini Kit (Qiagen) according to the manufacturer's protocols. RNA was reverse transcribed to cDNA using the SuperScript VILO cDNA Synthesis Kit and Master Mix (Life Technologies). Gene expression was quantified using the SYBR Green method with TB Green® Fast qPCR Mix (TaKaRa Bio Inc., Shiga, Japan) and human and murine PSAP primers (TaKaRa Bio Inc.).

2.7 | ELISA

An anti-PSAP antibody was dispensed into a plate and incubated at a concentration of 0.5 mg/well for 1 day at 4°C for coating. After immobilization, the cell culture supernatants were applied to the plate and then reacted for 1 h at room temperature. The detect antibody was incubated for 30 min at room temperature. The absorbance of the solution was measured at 450 nm.

2.8 | Proliferation assay

At 24 h after siRNA transfection, the cells were detached and seeded for a proliferation assay. Cell proliferation was evaluated using Cell Count Reagent SF (Nacalai Tesque), according to the manufacturer's protocol. The absorbance value at 450 nm was measured to determine cell viability using a plate reader (Bio-Rad Laboratories).

2.9 | Wound healing assay

At 24 h after siRNA transfection, cells were detached and seeded for a wound healing assay in a culture-insert 2 Well in a μ-Dish 35 mm (81176, Ibidi). The cell monolayer was then scratched to introduce a gap as per the manufacturer's protocol. At 24 h after scratching, the cell uncovered areas (gaps) were visualized by microscopy and analyzed using ImageJ software version 1.53 (National Institute of Mental Health).

2.10 | Patient samples and ethical considerations

Human PDAC resected samples were harvested from 133 consecutive patients who had undergone radical pancreatectomy at the Department of General Surgery, Chiba University Hospital, between January 2013 and December 2015. Only samples that were histologically confirmed as primary invasive PDAC were included in the present study. Patients who died perioperatively or distant metastases at the time of resection were excluded. Tumor volume was calculated using the following formula: $\pi/6 \times (L \times W \times W)$, where L is the long diameter and W is the short diameter. The 8th edition of the UICC was applied to determine the TNM classification. The study protocol (protocol #2155) was approved by the ethics committee of

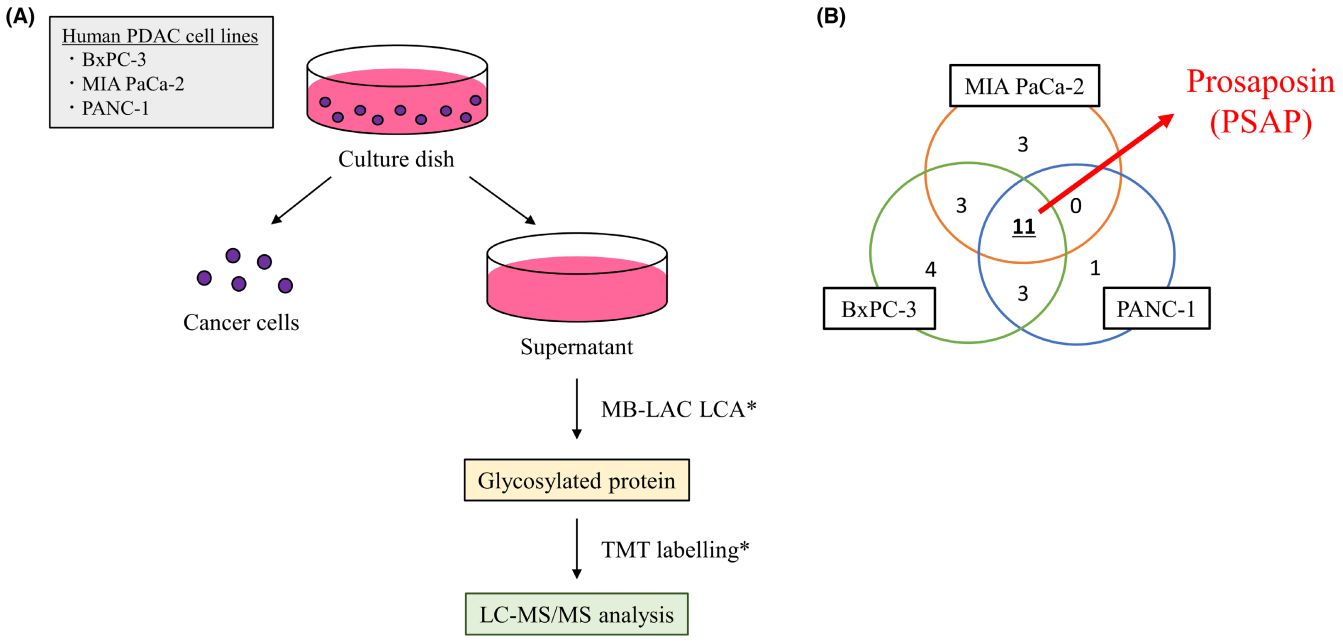

FIGURE 1 Identification of glycosylated proteins through an exhaustive secretome analysis of culture supernatants from three PDAC cell lines. (A) Experimental setup to identify glycosylated proteins. (B) Number of glycosylated proteins identified in the cell lines. MB-LAC LCA, magnetic bead lectin affinity chromatography *Lens culinaris* agglutinin; TMT labeling, tandem mass tag labeling; LC–MS/MS, liquid chromatography–tandem mass spectrometry

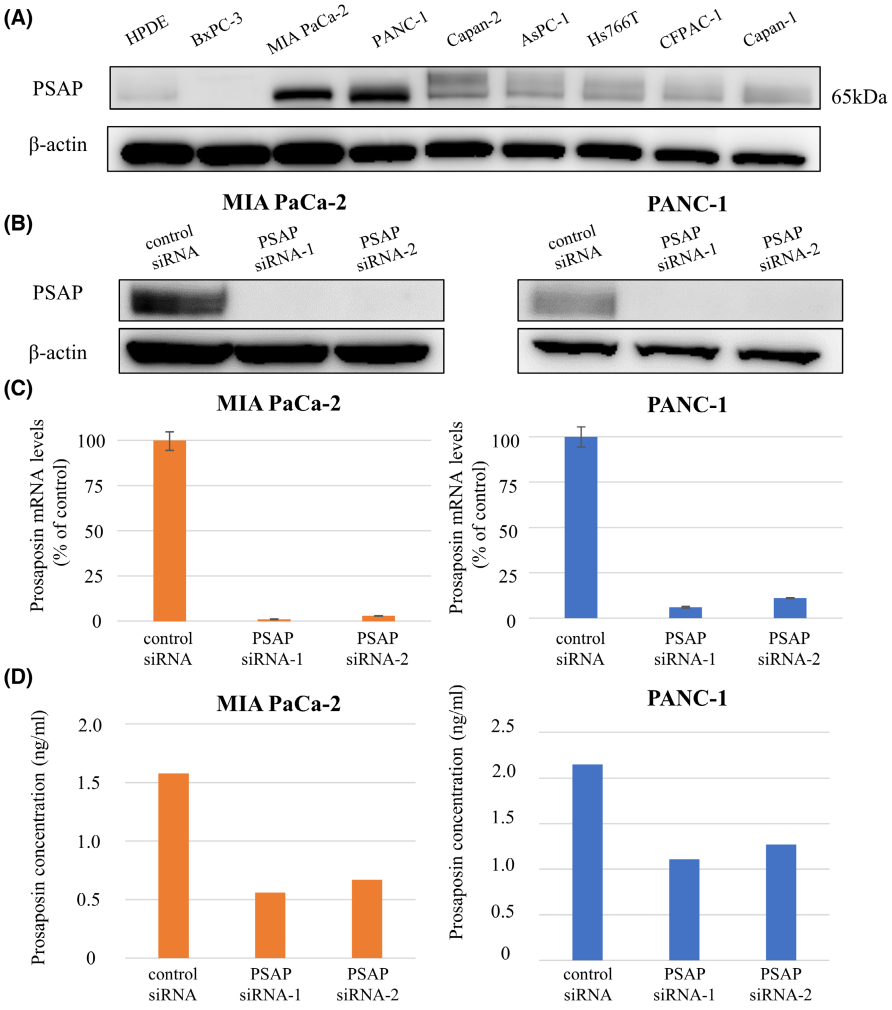

FIGURE 2 Prosaposin (PSAP) expression in cell lines and cell culture supernatants. (A) Western blot analysis of PSAP expression in human pancreatic duct epithelial (HPDE) cells, and PDAC cell lines derived from primary tumors (BxPC-3, MIA PaCa-2, PANC-1, Capan-2), metastatic ascites (AsPC-1), lymph node metastasis (Hs766T), and PDAC liver metastases (CFPAC-1, Capan-1). (B, C) Knockdown validation for PSAP-specific siRNA in cell lysates by western blot and quantitative PCR. (D) PSAP expression levels in cell culture supernatant, quantified by ELISA. Endogenous PSAP knockdown decreases PSAP secretion in cell culture supernatant

Chiba University, and written informed consent was obtained from each patient before surgery. Informed consents for PBMCs from healthy volunteers were also obtained.

2.11 | Immunohistochemistry and immunofluorescence staining

Immunohistochemistry and immunofluorescence staining were performed using 4-μm thick sections from formalin-embedded tissue blocks. Antigen retrieval was performed by autoclaving, and endogenous peroxidase activity was inactivated using 3% hydrogen peroxide. Nonspecific protein blocking was performed using 5% BSA. The sections were incubated overnight with primary antibodies at 4°C. Subsequently, the appropriate secondary antibodies were applied for 30 min at room temperature, followed by staining with diaminobenzidine (Nacalai Tesque). The antibody information is listed in Table S1. The histology of each human PDAC sample was examined by two independent investigators. The PSAP staining patterns were scored by multiplication based on the intensity of tumor cytoplasm (1: no to very weak staining, 2: weak staining, 3: strong staining, 4: very strong staining) and the proportion of positively stained tumor cells (1: <25%, 2:25–50%, 3:50–75%, 4:>75%). The number of $CD8^+$ T cells was manually counted in the tumor stroma and an average count from five different high-power fields (magnification, ×400) was taken.

2.12 | Isolation and culture protocols of PBMCs

Peripheral blood obtained from healthy volunteers was overlaid on Ficoll-Paque PLUS (Cytiva) and centrifuged to isolate PBMCs. Cells were incubated for 3 days in RPMI 1640 medium (Thermo Fisher Scientific) with 10% FBS and antibiotics. Con A (Nacalai Tesque) at a final concentration of 5 μg/ml was supplemented as a T-cell mitogen, and rhPSAP (16224-H08H, SinoBio) was used for stimulation at a concentration of 1000 ng/ml.

2.13 | Flow cytometry analysis

Incubated cells were centrifuged and resuspended in PBS with the relevant antibodies for 60 min. The antibodies used are detailed in Table S1. Flow cytometry analysis was performed using a CANTO II system (Beckton-Dickinson). The collected data were analyzed using

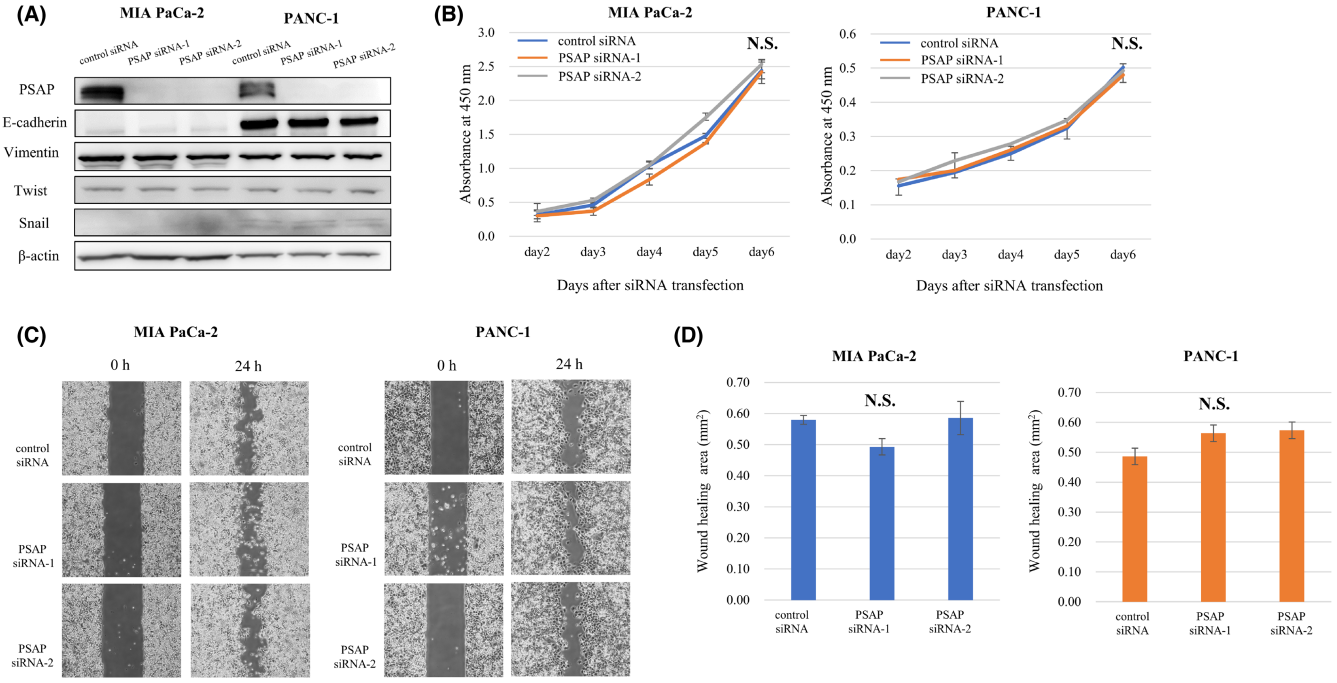

FIGURE 3 Knockdown of endogenous PSAP expression did not affect epithelial-to-mesenchymal transition, proliferation, and migration capacity in PDAC cells. (A) Expression levels of E-cadherin, vimentin, Twist, and Snail. (B) Proliferation assay comparing the control siRNA and PSAP-specific siRNA groups. (C) Representative image of migration assay. (D) Quantitative analyses of gap areas after scratching

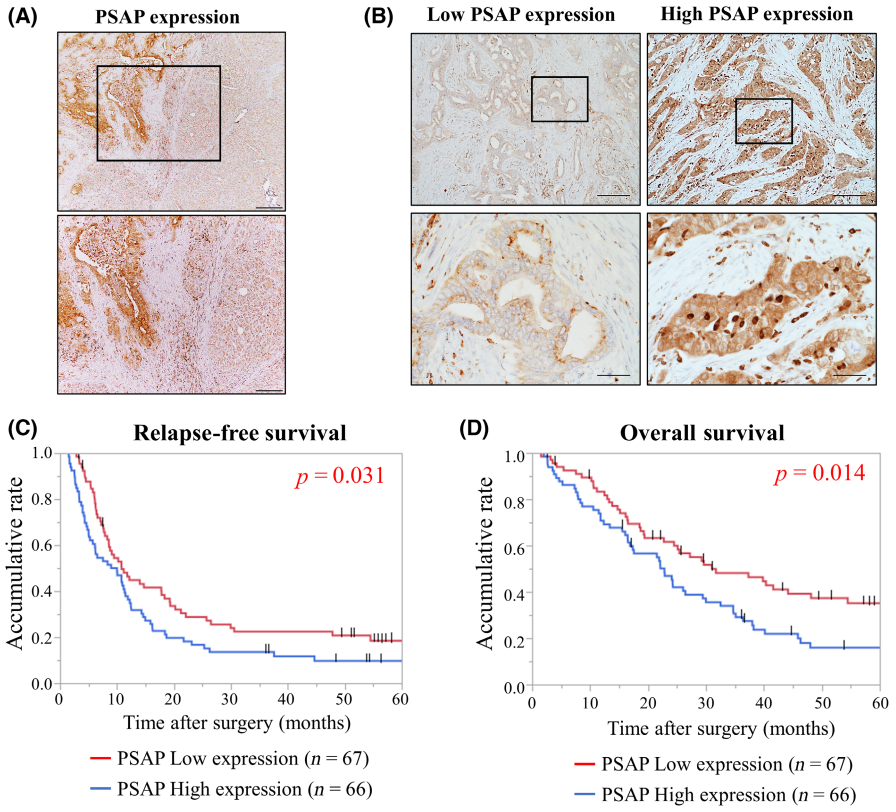

FIGURE 4 Immunohistochemistry of prosaposin (PSAP) expression in resected PDAC tissues. (A, B) Representative immunohistochemistry staining for PSAP in resected PDAC tissues. Original magnification: (A) upper panels ×100 (scale bars, 200 μm), lower panels ×200 (scale bar, 100 μm); (B) upper panels ×100 (scale bars, 200 μm), lower panels ×400 (scale bars, 50 μm). (C, D) Kaplan–Meier analyses of patients with high PSAP expression versus low PSAP expression for relapse-free survival (C) and overall survival (D). The high PSAP expression group showed significantly poorer relapse-free survival ($p = 0.031$, log-rank test) and overall survival ($p = 0.014$, log-rank test) compared with the low PSAP group

FlowJo v10.8.1 software (Beckton-Dickinson). Flow cytometric gating was performed by identifying the viable lymphocytes using side and forward scatters. After further gating for CD3, the percentages of $CD4^+$ and $CD8^+$ cells were calculated.

2.14 | Orthotopic transplantation model

Female C57BL/6 mice (CLEA Japan) aged 8–10 weeks were injected with 2×10^5 PKCY cells suspended in 25 μl medium into the

TABLE 1 Characteristics of PDAC patients for PSAP expression in IHC analysis

	PSAP expression		
	Low ($n = 67$)	High ($n = 66$)	p-Value
Age (mean ± SD)	65.6 ± 1.3	66.3 ± 1.3	0.714
Gender (male/female)	32/35	36/30	0.271
Tumor location (head/body, tail)	46/21	48/18	0.373
Resectability (R/BR,UR)[a]	41/26	39/27	0.472
Neoadjuvant therapy (+/−)	28/39	30/36	0.401
Tumor volume (median [IQR])	4750 (2827–8109)	7225 (4196–11,550)	0.029*
pT stage (T3,4/T1,2)[a]	51/16	44/22	0.155
pN stage (N0/N1,2)[a]	19/48	15/51	0.293
Histological grade (G3/G1,2)	8/59	8/58	0.592
Curability (R0/R1,2)	49/18	41/25	0.121
Adjuvant chemotherapy (+/−)	49/18	45/21	0.793
(Fisher's exact test)			

Abbreviations: IHC, immunohistochemistry; IQR, interquartile range; p, pathological findings; PDAC, pancreatic ductal adenocarcinoma; PSAP, prosaposin; SD, standard deviation.

[a]The Union for International Cancer Control 8th edition.

*Significant value ($p < 0.05$).

TABLE 2 Recurrence site divided by PSAP expression in IHC analysis

	PSAP expression		
	Low ($n = 52$)	High ($n = 59$)	p-Value
Liver metastasis (+/−)	11/41	23/36	0.033*
Lung metastasis (+/−)	9/43	9/50	0.710
Peritoneal recurrence (+/−)	10/42	10/49	0.713
Local recurrence (+/−)	27/25	27/32	0.799
(Fisher's exact test)			

*Significant value ($p < 0.05$).

Abbreviations: IHC, immunohistochemistry; PSAP, prosaposin.

subcapsular region of the pancreas under anesthesia. After injection, a sterile cotton swab was immediately placed at the injection site to prevent the spread of cancer cells into the abdominal free space. The mice were sacrificed 30 days after transplantation for histological analysis. For details, please refer to a previous study.[26] Paraffin-embedded pancreata were cut into 4 μm thick section, 200 μm apart from each other, followed by staining with hematoxylin and eosin (H&E). Slides with the maximum tumor area were used to measure the tumor size under a microscope. Tumor volume was calculated using the same formula as for the human specimens. The number of $CD8^+$ T cells was counted in two different high-power fields. All animal experiments in the present study were performed humanely. The studies were carried put according to a protocol approved by the Committee of Animal Welfare of Chiba university.

2.15 | Statistical analysis

Statistically significant differences were determined using Welch's *t*-test, Mann–Whitney–Wilcoxon test, chi-squared test, and Fisher's exact test. Cumulative survival rates were calculated using the Kaplan–Meier method, and the significance of the difference was evaluated using the log-rank test. Cox proportional hazard models were used for univariate and multivariate survival analyses. Statistical significance was set at $p < 0.05$. Data from in vitro experiments were independently performed at least three times. All statistical analyses were performed using JMP Pro version 15.0.0 (SAS Institute Inc.).

3 | RESULTS

3.1 | Identification of PSAP by TMT labeling and LC–MS/MS analysis

To identify PDAC-related glycoproteins, TMT labeling and LC–MS/MS were used to analyze proteins extracted from the culture media of three PDAC cell lines (BxPC-3, MIA PaCa-2, and PANC-1) in secretome analyses (Figure 1A). In total, 25 glycoproteins were identified, and 11 proteins of these overlapped across the three cell lines (Figure 1B; Table S2). Of these candidates, PSAP is widely known as an essential neurotrophic factor in nerve systems.[18,19] In addition, several neurotrophic factors have been demonstrated to affect PDAC progression.[27–29] Therefore, we hypothesized that PSAP could be involved in cancer progression and selected it for further analyses regarding its functional contributions in the TME of PDAC.

TABLE 3 Univariate and multivariate analyses for overall survival in PDAC

		Univariate analysis		Multivariate analysis	
	$n = 133$	Hazard ratio (95%CI)	p-Value	Hazard ratio (95%CI)	p-Value
Age (years, ≥/<65)	82/51	1.05 (0.54–2.02)	0.893		
Gender (male/female)	68/65	1.04 (0.70–1.55)	0.843		
Resectability (BR,UR/R)[a]	53/80	1.92 (1.28–2.87)	<0.001*	1.54 (0.98–2.43)	0.064
Neoadjuvant therapy (+/−)	58/75	1.24 (0.30–0.83)	0.296		
Tumor volume (≥/<575)[b]	64/69	2.02 (1.35–3.05)	<0.001*	1.30 (0.80–2.11)	0.290
pT stage (T3,4/T1,2)[a]	38/95	1.71 (1.12–2.61)	0.013*	1.03 (0.62–1.69)	0.922
pN stage (N1,2/N0)[a]	99/34	2.39 (1.47–4.08)	0.008*	2.46 (1.44–4.20)	0.001*
Curability (R1,R2/R0)	45/88	1.42 (0.94–2.16)	0.065		
Histological grade (G3/G1,2)	16/117	1.05 (0.51–1.92)	0.894		
Adjuvant chemotherapy (+/−)	73/60	0.58 (0.38–0.90)	0.015*	0.52 (0.32–0.82)	0.005*
PSAP expression (high/low)	76/57	1.654 (1.11–2.48)	0.014*	1.58 (1.04–2.40)	0.031*
(Cox proportional hazard models)					

Abbreviations: CI, confidence interval; p, pathological findings; PDAC, pancreatic ductal adenocarcinoma; PSAP, prosaposin; SD, standard deviation.

[a]The Union for International Cancer Control 8th edition.

[b]Tumor volume was divided according to the median value, 5575 mm^3.

*Significant value ($p < 0.05$).

3.2 | PSAP expression in human PDAC cell lines and cell culture supernatants

We investigated PSAP expression in HPDE cells and eight PDAC cell lines using western blot analysis. PSAP was highly expressed in most of primary and metastatic PDAC cell lines (Figure 2A). Among them, we selected MIA PaCa-2 and PANC-1 for further in vitro experiments to assess the functional roles of PSAP because these two PDAC cell lines were derived from primary PDAC tumor cells and highly expressed in those cell lysates. Then, we observed endogenous PSAP expression was decreased in PSAP-knockdown cells prepared by transfection with PSAP-specific siRNAs (Figure 2B,C). To determine whether PSAP secretion corresponded to endogenous expression in PDAC cells, we measured the PSAP concentration in PDAC cell culture supernatants. The ELISA results revealed that PSAP knockdown decreased PSAP expression in the supernatant (Figure 2D). These data suggested that PSAP is highly expressed in PDAC cells.

3.3 | PSAP knockdown did not affect proliferation and migration in PDAC cells

We next examined whether the knockdown of endogenous PSAP in PDAC cells using PSAP-specific siRNAs altered their cellular phenotype, and their capacity for proliferation and migration. PSAP knockdown did not alter the expression of EMT markers in MIA PaCa-2 and PANC-1 cells (Figure 3A). Moreover, no significant difference was observed in the proliferation and migration abilities between PSAP-knockdown cells and control cells in these two PDAC cell lines (Figure 3B–D). Additionally, we conducted extrinsic PSAP supplementation to PDAC cells to assess cell proliferation capacity. Similar to the knockdown experiments, PSAP supplementation did not act on cell proliferation in MIA PaCa-2 and PANC-1 cells (Figure S1). These data suggested that intrinsic PSAP expression is not associated with cell proliferation and EMT properties in PDAC cells in vitro.

3.4 | High PSAP expression in PDAC tissues is correlated with poor prognosis of patients

To assess the correlation between PSAP and clinicopathological features, we examined PSAP expression in resected PDAC tissues using IHC. PSAP was predominantly expressed in the tumor cytoplasm and the immune cells surrounding PDAC cells, but weakly expressed in the acinar cells (Figure 4A). All patients were divided into two groups according to their staining scores (refer to Materials and Methods). In total, 67 patients (50.4%) were classified in the low PSAP expression group, whereas 66 patients (49.6%) were classified in the high PSAP expression group (Figure 4B). The clinicopathological features of patients with PDAC based on PSAP expression are shown in Table 1. Interestingly, the high PSAP group showed significantly larger tumor volumes compared with the low PSAP group ($p = 0.029$), whereas no significant differences were observed in other factors. Regarding the recurrence site patterns, liver metastasis was observed more frequently in the high PSAP group than in the low PSAP group ($p = 0.033$) (Table 2). Kaplan–Meier analysis revealed that the high PSAP group had significantly shorter relapse-free survival ($p = 0.031$) (Figure 4C) and overall survival ($p = 0.014$) compared with those in the low PSAP group (Figure 4D). Furthermore, high PSAP expression was an independent prognostic factor for overall survival in multivariate analysis using Cox proportional hazard models ($p = 0.031$) (Table 3). These clinical data indicated that

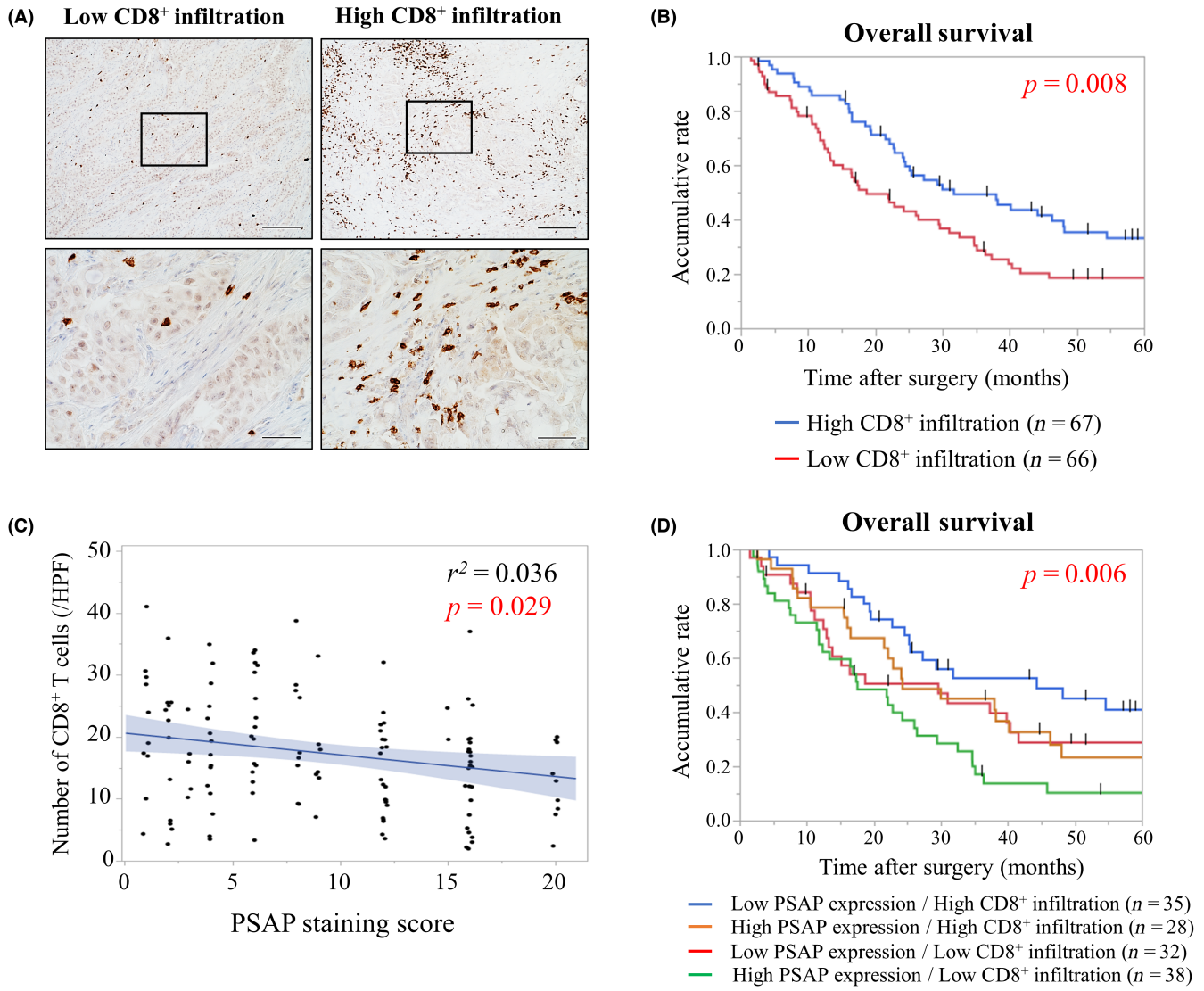

FIGURE 5 Immunohistochemistry of $CD8^+$ T cells and PSAP in resected PDAC tissues. (A) Representative immunohistochemistry staining for $CD8^+$ T cells in resected PDAC tissues. Original magnification: upper panels ×100 (scale bars, 200 μm), lower panels ×400 (scale bars, 50 μm). (B) Kaplan–Meier analysis for overall survival based on $CD8^+$ T-cell infiltration. (C) Correlation between number of $CD8^+$ T cells and PSAP expression. PSAP expression was inversely correlated with the number of infiltrated $CD8^+$ T cells in the cancer-surrounding stroma ($R^2 = 0.036$, $p = 0.029$). (D) Kaplan–Meier analysis of patients with PSAP expression and $CD8^+$ T-cell infiltration. Patients with high PSAP expression and low $CD8^+$ T-cell counts presented significantly poorer survival than did other patients ($p = 0.006$, log-rank test)

high PSAP expression is associated with poor prognosis and recurrence of liver metastasis in patients with PDAC.

3.5 | $CD8^+$ infiltrating T cells were negatively correlated with PSAP expression in resected PDAC tissues

Antitumor immunity is considered one of the most important factors that greatly influences the prognosis of patients with malignancies. In particular, $CD8^+$ T cells are regarded as TILs, which are crucial components of antitumor immunity. To evaluate whether PSAP influences $CD8^+$ T-cell infiltration in the TME of PDAC, we assessed the correlation between PSAP expression and $CD8^+$ T cells in resected PDAC tissues. First, the sample cohort was divided into high and low $CD8^+$ cell infiltration groups by the median value to assess the correlation between TIL infiltration and clinicopathological factors (Figure 5A). Among the various perioperative parameters, patients with decreased $CD8^+$ T cells showed significantly larger tumor volumes than those with enriched $CD8^+$ T cells ($p = 0.012$) (Table S3). The low $CD8^+$ cell infiltration group showed poorer prognosis than the high $CD8^+$ cell infiltration group ($p = 0.008$) (Figure 5B). Notably, the number of $CD8^+$ T cells in the periphery of cancer cells demonstrated a significant negative correlation with PSAP expression ($R^2 = 0.036$, $p = 0.029$) (Figure 5C). In prognosis, both high and low $CD8^+$ cell infiltration groups demonstrated the

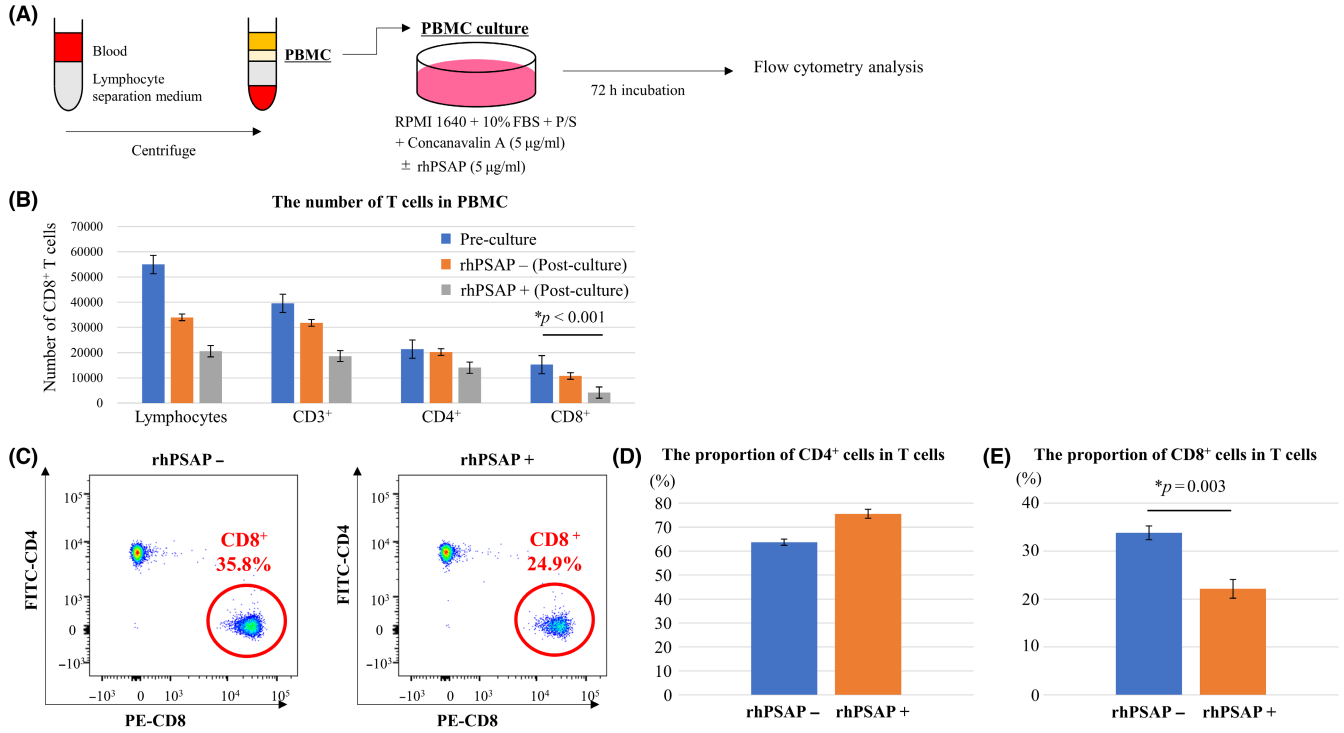

FIGURE 6 Stimulation of human peripheral blood monocyte cells (PBMCs) using recombinant prosaposin (rhPSAP). (A) PBMC culture protocol. (B) The number of T cells in PBMCs before and after culture, and with and without rhPSAP. The number of $CD8^+$ cells was significantly decreased by cell culturing and PSAP supplementation. (C) Representative scatter plots for $CD4^+$ and $CD8^+$ cells in the rhPSAP-unstimulated and rhPSAP-stimulated groups. (D, E) Percentages of $CD4^+$ (D) and $CD8^+$ (E) cells among the $CD3^+$ cells in each group. The proportion of $CD8^+$ cells was significantly decreased by PSAP stimulation ($p = 0.003$, Welch's *t*-test). All values are presented as the mean ± standard error of the mean (SEM)

worst prognosis compared with the other groups of patients with PDAC ($p = 0.006$) (Figure 5D). In a previous study, PSAP has been reported to activate myeloid-derived suppressor cells (MDSCs) and macrophages, therefore we performed immunofluorescence staining to confirm that immune cells expressed PSAP.[21,30] We found certain subsets of immune cells in which PSAP were co-expressed with CD11b or CD163, indicating PSAP is expressed in MDSCs and M2 macrophages. (Figure S2). This finding may suggest that PSAP have the function of not just reducing the number of $CD8^+$ T cells, but also affecting the expression of other suppressor cells. These data implicated that PSAP suppresses TILs in the TME, resulting in poor outcomes in patients with PDAC.

3.6 | PSAP stimulation decreased the proportion of $CD8^+$ T cells in PBMCs in vitro

To elucidate the effect of PSAP on immune cells, we evaluated the changes in the proportion of lymphocyte subsets using flow cytometry by stimulating PBMCs with rhPSAP (Figure 6A). PBMCs extracted from human blood are composed of various immune cells subsets such as T cells, B cells, monocytes, and dendritic cells. Flow cytometry analyses revealed that the number of living lymphocytes were decreased, but the proportion of $CD3^+$ T cells was increased in PBMCs culture stimulated with Con A (Figure 6B). We also observed the culture had decrease $CD8^+$ T cells (Figure 6B). Notably, the rhPSAP-treated group showed significantly smaller proportions of $CD8^+$ T cells in the $CD3^+$ cells compared with the rhPSAP-untreated group ($p = 0.003$) (Figure 6C–E). These results suggested that PSAP stimulation suppressed the proportion of $CD8^+$ T cells in PBMCs in in vitro culture experiment.

3.7 | PSAP suppression facilitates TILs in the TME of PDAC in vivo

To investigate the functional contribution of PSAP to PDAC progression in vivo, we conducted orthotopic transplantation by injecting PKCY cells into mice (Figure 7A). PSAP knockdown with PSAP shRNAs was confirmed by western blot analysis and quantitative RT-PCR (Figure 7B, Figure S3A). Consistent with the results in human PDAC cells, no significant differences were observed in the proliferation and migration of murine PDAC cells (Figure S3B–D). At 30 days after cell injection, the experimental mice were sacrificed to assess the tumor volume and number of TILs (Figure S4B). Interestingly, the number of $CD8^+$ T cells in the PSAP shRNA group was significantly higher than that in the control shRNA group (Figure 7C,D). Furthermore, tumor volumes in the PSAP shRNA group were

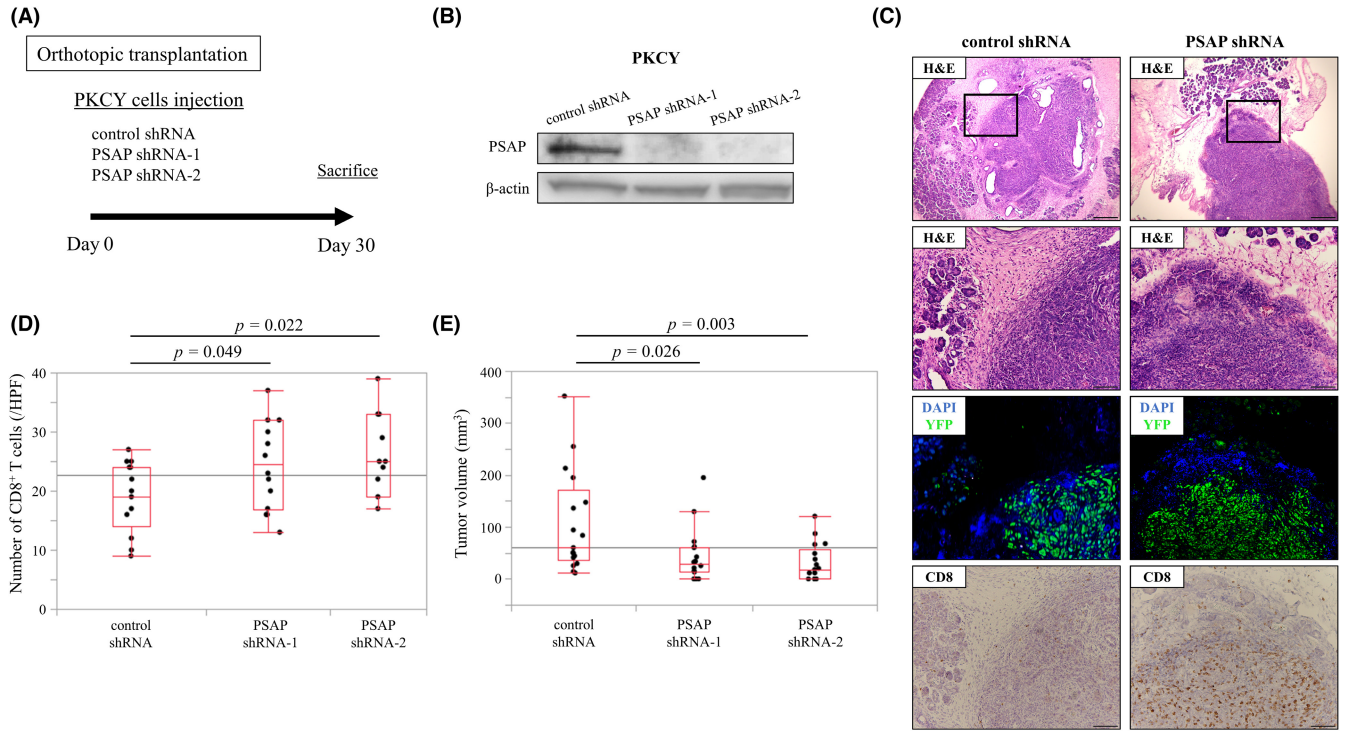

FIGURE 7 Orthotopic transplantation model using C57BL/6 and murine PDAC cells (KPCY mice; *Pdx1-cre*; *LSL-Kras*$^{G12D/+;p53fl/+}$; *R26*^{YFP} mice). (A) Schema of the orthotopic transplantation model. (B) Validation of PSAP knockdown using PSAP-specific shRNA by western blot. (C) Representative images of tumor histology in the orthotopic transplantation model by H&E staining ×40 magnification (scale bar, 400 μm) and ×200 magnification (scale bar, 100 μm) and double immunofluorescence staining for yellow fluorescent protein (YFP) (green) and DAPI (blue) in the primary tumor. Upper panels: a case from the control shRNA group. Lower panels: a case from the PSAP shRNA-2 group. (D) Box plots of CD8$^+$ T-cell infiltration in the three groups. Box plots show the mean, median, and the 25th and 75th percentiles. PSAP shRNA groups showed smaller tumors than those in the control shRNA group (control shRNA vs. PSAP shRNA-1: $p = 0.026$; control shRNA vs. PSAP shRNA-2: $p = 0.003$). (E) Box plots of tumor volumes in the three groups. PSAP shRNA groups showed higher infiltration of CD8$^+$ cells than those in the control shRNA group (control shRNA vs. PSAP shRNA-1: $p = 0.049$; control shRNA vs. PSAP shRNA-2: $p = 0.022$, Mann–Whitney–Wilcoxon test)

significantly smaller than those in the control shRNA group, with no differences in body weight between these two groups (Figure 7E, Figure S4C). These results suggested that PSAP promotes cancer progression by decreasing the number of TILs in vivo.

4 | DISCUSSION

In this study, we demonstrated that PSAP, which was identified in the secretion of PDAC cells using a comprehensive proteomic approach, suppressed antitumor immunity by decreasing TILs, leading to PDAC progression. We further found that high PSAP expression in clinical PDAC samples was associated with large tumor volumes and low infiltration of CD8$^+$ T cells, resulting in the poor prognosis of patients with PDAC. In an in vitro experiment, PSAP stimulation in PBMCs induced a decrease in the number of CD8$^+$ T cells. Moreover, PSAP knockdown increased CD8$^+$ T-cell infiltration and tumor shrinkage in an orthotopic transplantation model. To our knowledge, this is the first study to demonstrate that PSAP facilitates cancer progression by decreasing TILs in the TME of PDAC.

PSAP acts as a precursor of saposins A–D, which mediate the hydrolysis of sphingolipids in lysosomes.[31,32] Recent studies have described the functional roles of PSAP as a secreted protein in cancer metastasis.[20–24] Ishihara and colleagues showed that PSAP secreted from fibroblasts in the stiff extracellular matrix affected mammary cancer cells and promoted cancer cell proliferation, but inhibited metastasis.[20] Interestingly, Raul and colleagues reported that metastasis-incompetent tumors secreted PSAP, which created a metastasis-refractory microenvironment by thrombospondin-1 production in bone marrow-derived Gr1$^+$ myeloid cells in prostate and breast cancers.[21] Contrary to these results, we observed that PSAP was associated with a high frequency of liver metastases after surgery in PDAC. This discrepancy may be caused by differences in the immunogenic tumor microenvironment among various cancers.

PSAP is also known to bind as a ligand to LRP-1 activating numerous cell signaling,[33] and TLR4 activating the NF-κB signaling pathway.[23] Both receptors are expressed in multiple cell types including dendritic cells and macrophages among immune cells. In line with this, we observed that PSAP expression was positively correlated with tumor growth in resected human PDAC tissues. Moreover, we

demonstrated that PSAP knockdown impaired the tumorigenicity of PDAC in vivo. We did not assess how PSAP suppressed $CD8^+$ T cells in the present study, however it could be speculated from the results and the published literature that PSAP may activate MDSCs and tumor-associated M2 macrophages by LRP1 and/or TLR4 through the identified signaling pathways.

Antitumor immunity is one of the crucial and physiological host responses in the defense against cancer progression. In particular, T-cell infiltration in the TME is a key phenomenon of antitumor immunity, resulting in tumor cell toxicity.[34,35] Immunotherapy has been administered as a treatment that facilitates TILs to recognize and attack cancer cells based on their unique antigens.[36] Some malignancies with tumor antigens accumulate TILs, which is a successful response to immunotherapy, whereas PDAC is characterized by low infiltration of intratumoral T cells,[37,38] and demonstrates an extremely limited response to immunotherapy.[11,39,40] In this study, we showed that PSAP decreased $CD8^+$ T cells in PBMCs and was negatively correlated with $CD8^+$ T-cell infiltration in PDAC. Therefore, PSAP promoted cancer progression by modulating the immunosuppressive condition of PDAC. The regulation of PSAP is supposed to enhance immunotherapy, including immune checkpoint blockade, by accumulating cytotoxic T cells. Combination therapy with PSAP-targeted immunotherapy could therefore provide a potentially powerful treatment option for PDAC.

This study has some inherent limitations. First, to explore the exact mechanism involved in the suppressive effect of PSAP on $CD8^+$ T-cell infiltration in the TME of PDAC, the canonical signaling pathway and the corresponding receptor need to be comprehensively analyzed. Second, metastasis assays such as intraportal vein injection have not been conducted to clarify the impact of PSAP function on liver metastasis in vivo. Additional studies are needed to elucidate the mechanism of PSAP through altered immunogenicity in the TME of PDAC. In conclusion, PSAP suppresses $CD8^+$ T-cell infiltration into the stroma surrounding the tumor, which results in PDAC progression. Further studies can help to determine whether these results can contribute to the establishment of an immunomodulating therapy for PDAC.

AUTHOR CONTRIBUTIONS

YM and ST designed the study; YM, KS, and SaT performed the research; ST and KS supervised the experiments; YM, ST, KS, SaT, KF, TT, SK, and MO discussed and analyzed the data; and YM and ST wrote the manuscript. All authors have read and approved the final manuscript.

ACKNOWLEDGMENTS

This study was supported by a Grant-in-Aid for Scientific Research (KAKENHI): "KIBAN" B: 19H03725 (ST, MO) and "KIBAN" C: 19K09113 (MO, ST, SK).

DISCLOSURE

The authors declare no conflicts of interest.

ORCID

Yoji Miyahara https://orcid.org/0000-0001-5636-2607
Shigetsugu Takano https://orcid.org/0000-0002-6495-0422

REFERENCES

1. Siegel RL, Miller KD, Jemal A. Cancer statistics, 2020. *CA Cancer J Clin*. 2020;70(1):7-30.
2. Ho WJ, Jaffee EM, Zheng L. The tumour microenvironment in pancreatic cancer - clinical challenges and opportunities. *Nat Rev Clin Oncol*. 2020;17(9):527-540.
3. Hosein AN, Brekken RA, Maitra A. Pancreatic cancer stroma: an update on therapeutic targeting strategies. *Nat Rev Gastroenterol Hepatol*. 2020;17(8):487-505.
4. Ene-Obong A, Clear AJ, Watt J, et al. Activated pancreatic stellate cells sequester CD8+ T cells to reduce their infiltration of the juxtatumoral compartment of pancreatic ductal adenocarcinoma. *Gastroenterology*. 2013;145(5):1121-1132.
5. Huber M, Brehm CU, Gress TM, et al. The immune microenvironment in pancreatic cancer. *Int J Mol Sci*. 2020;21(19).
6. Topalian SL, Hodi FS, Brahmer JR, et al. Safety, activity, and immune correlates of anti-PD-1 antibody in cancer. *N Engl J Med*. 2012;366(26):2443-2454.
7. Brahmer JR, Drake CG, Wollner I, et al. Phase I study of single-agent anti-programmed death-1 (MDX-1106) in refractory solid tumors: safety, clinical activity, pharmacodynamics, and immunologic correlates. *J Clin Oncol*. 2010;28(19):3167-3175.
8. Robert C, Long GV, Brady B, et al. Nivolumab in previously untreated melanoma without BRAF mutation. *N Engl J Med*. 2015;372(4):320-330.
9. Borghaei H, Paz-Ares L, Horn L, et al. Nivolumab versus docetaxel in advanced nonsquamous non-small-cell lung cancer. *N Engl J Med*. 2015;373(17):1627-1639.
10. Leinwand J, Miller G. Regulation and modulation of antitumor immunity in pancreatic cancer. *Nat Immunol*. 2020;21(10):1152-1159.
11. Balachandran VP, Beatty GL, Dougan SK. Broadening the impact of immunotherapy to pancreatic cancer: challenges and opportunities. *Gastroenterology*. 2019;156(7):2056-2072.
12. Majidpoor J, Mortezaee K. The efficacy of PD-1/PD-L1 blockade in cold cancers and future perspectives. *Clin Immunol*. 2021;226:108707.
13. Pinho SS, Reis CA. Glycosylation in cancer: mechanisms and clinical implications. *Nat Rev Cancer*. 2015;15(9):540-555.
14. Stowell SR, Ju T, Cummings RD. Protein glycosylation in cancer. *Annu Rev Pathol*. 2015;10:473-510.
15. Läubli H, Borsig L. Altered cell adhesion and glycosylation promote cancer immune suppression and metastasis. *Front Immunol*. 2019;10:2120.
16. Mereiter S, Balmaña M, Campos D, Gomes J, Reis CA. Glycosylation in the era of cancer-targeted therapy: where are we heading? *Cancer Cell*. 2019;36(1):6-16.
17. Tsuchida S, Satoh M, Kawashima Y, et al. Application of quantitative proteomic analysis using tandem mass tags for discovery and identification of novel biomarkers in periodontal disease. *Proteomics*. 2013;13(15):2339-2350.
18. Nicholson AM, Finch NA, Almeida M, et al. Prosaposin is a regulator of progranulin levels and oligomerization. *Nat Commun*. 2016;7:11992.
19. O'Brien JS, Carson GS, Seo HC, Hiraiwa M, Kishimoto Y. Identification of prosaposin as a neurotrophic factor. *Proc Natl Acad Sci USA*. 1994;91(20):9593-9596.
20. Ishihara S, Inman DR, Li WJ, Ponik SM, Keely PJ. Mechano-signal transduction in mesenchymal stem cells induces prosaposin secretion to drive the proliferation of breast cancer cells. *Cancer Res*. 2017;77(22):6179-6189.

21. Catena R, Bhattacharya N, El Rayes T, et al. Bone marrow-derived Gr1+ cells can generate a metastasis-resistant microenvironment via induced secretion of thrombospondin-1. *Cancer Discov*. 2013;3(5):578-589.
22. Kang SY, Halvorsen OJ, Gravdal K, et al. Prosaposin inhibits tumor metastasis via paracrine and endocrine stimulation of stromal p53 and Tsp-1. *Proc Natl Acad Sci USA*. 2009;106(29):12115-12120.
23. Jiang Y, Zhou J, Luo P, et al. Prosaposin promotes the proliferation and tumorigenesis of glioma through toll-like receptor 4 (TLR4)-mediated NF-κB signaling pathway. *EBioMedicine*. 2018;37:78-90.
24. Wu Y, Sun L, Zou W, et al. Prosaposin, a regulator of estrogen receptor alpha, promotes breast cancer growth. *Cancer Sci*. 2012;103(10):1820-1825.
25. Sogawa K, Takano S, Iida F, et al. Identification of a novel serum biomarker for pancreatic cancer, C4b-binding protein α-chain (C4BPA) by quantitative proteomic analysis using tandem mass tags. *Br J Cancer*. 2016;115(8):949-956.
26. Sasaki K, Takano S, Tomizawa S, et al. C4b-binding protein α-chain enhances antitumor immunity by facilitating the accumulation of tumor-infiltrating lymphocytes in the tumor microenvironment in pancreatic cancer. *J Exp Clin Cancer Res*. 2021;40(1):212.
27. Saloman JL, Singhi AD, Hartman DJ, Normolle DP, Albers KM, Davis BM. Systemic depletion of nerve growth factor inhibits disease progression in a genetically engineered model of pancreatic ductal adenocarcinoma. *Pancreas*. 2018;47(7):856-863.
28. Ceyhan GO, Giese NA, Erkan M, et al. The neurotrophic factor artemin promotes pancreatic cancer invasion. *Ann Surg*. 2006;244(2):274-281.
29. Ito Y, Okada Y, Sato M, et al. Expression of glial cell line-derived neurotrophic factor family members and their receptors in pancreatic cancers. *Surgery*. 2005;138(4):788-794.
30. van Leent MMT, Beldman TJ, Toner YC, et al. Prosaposin mediates inflammation in atherosclerosis. *Sci Transl Med*. 2021;13(584):eabe1433.
31. O'Brien JS, Kishimoto Y. Saposin proteins: structure, function, and role in human lysosomal storage disorders. *FASEB J*. 1991;5(3):301-308.
32. Morimoto S, Martin BM, Yamamoto Y, Kretz KA, O'Brien JS, Kishimoto Y. Saposin A: second cerebrosidase activator protein. *Proc Natl Acad Sci USA*. 1989;86(9):3389-3393.
33. Gonias SL, Campana WM. LDL receptor-related protein-1: a regulator of inflammation in atherosclerosis, cancer, and injury to the nervous system. *Am J Pathol*. 2014;184(1):18-27.
34. St Paul M, Ohashi PS. The roles of CD8(+) T cell subsets in antitumor immunity. *Trends Cell Biol*. 2020;30(9):695-704.
35. Farhood B, Najafi M, Mortezaee K. CD8(+) cytotoxic T lymphocytes in cancer immunotherapy: a review. *J Cell Physiol*. 2019;234(6):8509-8521.
36. Yang Y. Cancer immunotherapy: harnessing the immune system to battle cancer. *J Clin Invest*. 2015;125(9):3335-3337.
37. Mortezaee K. Enriched cancer stem cells, dense stroma, and cold immunity: interrelated events in pancreatic cancer. *J Biochem Mol Toxicol*. 2021;35(4):e22708.
38. Mortezaee K, Najafi M. Immune system in cancer radiotherapy: resistance mechanisms and therapy perspectives. *Crit Rev Oncol Hematol*. 2021;157:103180.
39. Mizrahi JD, Surana R, Valle JW, Shroff RT. Pancreatic cancer. *Lancet*. 2020;395(10242):2008-2020.
40. O'Reilly EM, Oh DY, Dhani N, et al. Durvalumab with or without Tremelimumab for patients with metastatic pancreatic ductal adenocarcinoma: a phase 2 randomized clinical trial. *JAMA Oncol*. 2019;5(10):1431-1438.

SUPPORTING INFORMATION

Additional supporting information may be found in the online version of the article at the publisher's website.

How to cite this article: Miyahara Y, Takano S, Sogawa K, et al. Prosaposin, tumor-secreted protein, promotes pancreatic cancer progression by decreasing tumor-infiltrating lymphocytes. *Cancer Sci*. 2022;113:2548-2559. doi: 10.1111/cas.15444